Substrate adaptability of β-lactamase

Sun, J.

Chapter 2

Enhanced activity against a third-generation cephalosporin by destabilization of the active site of a class A beta-lactamase

Based on the research article:

Sun, J., Chikunova, A., Boyle, A. L., Voskamp, P., Timmer, M., & Ubbink, M. (2023). Enhanced activity against a third-generation cephalosporin by destabilization of the active site of a class A beta-lactamase. *International Journal of Biological Macromolecules*, *250*, 126160.

Abstract

The β-lactamase BlaC conveys resistance to a broad spectrum of β-lactam antibiotics to its host *Mycobacterium tuberculosis* but poorly hydrolyzes third generation cephalosporins, such as ceftazidime. Variants of other β-lactamases have been reported to gain activity against ceftazidime at the cost of the native activity. To understand this trade-off, laboratory evolution was performed, screening for enhanced ceftazidime activity. The variant BlaC Pro167Ser shows faster breakdown of ceftazidime, poor hydrolysis of ampicillin and only moderately reduced activity against nitrocefin. NMR spectroscopy, crystallography and kinetic assays demonstrate that the resting state of BlaC P167S exists in an open and a closed state. The open state is more active in the hydrolysis of ceftazidime. In this state the catalytic residue Glu166, generally believed to be involved in the activation of the water molecule required for deacylation, is rotated away from the active site, suggesting it plays no role in the hydrolysis of ceftazidime. In the closed state, deacylation of the BlaC-ceftazidime adduct is slow, while hydrolysis of nitrocefin, which requires the presence of Glu166 in the active site, is barely affected, providing a structural explanation for the trade-off in activities.

Introduction

A major cause of antibiotic resistance worldwide is the hydrolytic inactivation of β-lactam drugs by β-lactamases.[97-99] Bacterial resistance to early β-lactam antibiotics led to the development of oxyimino-cephalosporin antibiotics. This class of antibiotics, which includes molecules such as ceftazidime and cefotaxime, were poor substrates for most β-lactamases due to the bulky C7β aminothiazole-oxyimino side chain that does not easily fit into the active site.[100] However, the selection pressure exerted by these antibiotics led to the evolution of extended-spectrum β-lactamases (ESBLs) that have increased activity against these antibiotics.[98,101]

Regions that are affected by mutations leading to the ESBL phenotype include the B3 β-chain (234 to 240, Ambler numbering[73]),[102-107] the oxyanion hole (residue 69),[108] and the Ω-loop (residues 164 to 179), which lines part of the active site.[106-113] The mutations cause widening of the active site,[111,114,115] or a conformational change of the enzyme during hydrolysis.[108] Substitutions at these positions have also been observed in clinical isolates[116] for ceftazidime resistance in TEM-1, SHV-1, CTX-M, and the Pen family. [100,117-125] The Ω-loop substitutions have been extensively studied for their impact on substrate specificity and resistance. Disruption of the salt bridge formed by Arg164 and Asp179,[126-129] located on opposite sides of the Ω-loop's "neck,"[130,131] enhances the flexibility of the Ω-loop, enabling the hydrolysis of extended-spectrum cephalosporins. Deletion or replacement of the amino acids of the Ω-loop for PenL (also known as PenA) β-lactamase,[132] and, specifically, the substitution at position 167 in PenL,[100] TEM,[133] and CTX-M β-lactamases[114,134] were also shown to increase the rate of hydrolysis of ceftazidime, due to changes in the conformation of the Ω-loop. Bowman and co-workers have studied the presence of cryptic pockets in TEM-1. In a recent study, they demonstrate that the presence of a cryptic pocket in β-lactamase correlates with increased hydrolysis of benzylpenicillin, suggesting that the opened form enhances activity against this substrate, whereas the closed form may be beneficial for cefotaxime activity.[95] Porter et al. (2019) also identified a cryptic pocket, in CTX-M-9 β-lactamase. Binding of a ligand in this pocket pushed the Ω-loop open and results in reduced nitrocefin activity.[135] Opening of the active site was

observed in CTX-M P167S for ceftazidime acylated enzyme, but not for the substrate bound form,[136] and the authors suggest that the open form results in a larger active site that allows for hydrolysis. Thus, improved ceftazidime activity requires a wider active site, which is accompanied by deterioration of the activity on penicillins and earlier generations of cephalosporins, indicating an activity trade-off between ceftazidime and other β-lactam compounds.[95,110,137] This trade-off relates to dynamics in the Ω-loop,[136,138,139] but the mechanistic reason remains unclear.[140]

BlaC is the ESBL encoded on the *Mycobacterium tuberculosis* (Mtb) chromosome. Like other serine β-lactamases, BlaC utilizes an active site serine residue (Ser70) to perform a nucleophilic attack to the carbonyl carbon of the β-lactam ring, leading to the formation of a covalent acyl-enzyme intermediate. Glu166 is responsible for activation of the water molecule that reacts with the covalent adduct, causing deacylation.[65,141,142] BlaC is a good penicillinase but has little activity against third-generation cephalosporins, such as ceftazidime.[72] In this study, we aimed to test whether the poor hydrolysis rate of ceftazidime by BlaC could be improved by laboratory evolution, and establish the consequences for substrate specificity and the structural reasons for a possible trade-off in activity. In line with work on other β-lactamases,[136,138] the mutant P167S was found to increase ceftazidime inactivation. With a combination of kinetic experiments, NMR spectroscopy and crystal structure determination, it was shown that the resting state enzyme exists in an open and a closed state; the open state being the more active one against ceftazidime. The structures suggest that the displacement of catalytic residue Glu166, part of the Ω-loop, is the reason for the trade-off in activity. Its location in the active site is essential for penicillinase activity, but not for the hydrolysis of ceftazidime.

Results and discussion

BlaC P167S displays increased ceftazidime resistance.

To determine whether the BlaC ceftazidime resistance could be enhanced, a *blaC* gene mutant library was generated by error-prone PCR and selection was performed by

screening for resistance to ceftazidime in a cellular assay using an *Escherichia coli* expression system at three temperatures (23 °C, 30 °C and 37 °C). Screening at 30 °C gave rise to the P167S mutation in combination with mutations F72Y, S99G, I105F, A205T, D240G, and C287Y. Genes encoding the single mutations were subsequently tested for conferring ceftazidime resistance. The BlaC P167S mutant yielded better resistance to ceftazidime than wild-type (WT) BlaC and the other mutants (Table S2.1). However, BlaC P167S exhibited a reduced capacity to hydrolyze ampicillin (Figure S2.1), indicating an evolutionary trade-off.[143] Recombinant production of BlaC P167S yielded a folded enzyme that showed a decrease in thermal stability of 5.6 ℃ compared to that of WT BlaC (Figure S2.2).

Ceftazidime hydrolysis shows a branched kinetic mechanism.

To evaluate the β-lactam resistance profile of BlaC P167S, the kinetic parameters were investigated and compared to those of WT BlaC (Table 2.1). Ampicillin and nitrocefin (Figure S2.3) hydrolysis were measured at different substrate concentrations and data were fitted to the Michaelis-Menten equation (eq. 2.5 See materials and methods). The catalytic efficiencies ($k_{\mathrm{cat}}/K_{\mathrm{M}}$) of WT enzyme for ampicillin and nitrocefin are $1.3 \pm 0.1 \times 10^5\ \mathrm{M^{-1}s^{-1}}$ and $5.6 \pm 0.6 \times 10^5\ \mathrm{M^{-1}s^{-1}}$ respectively, in line with previously reported values.[72,144] The BlaC P167S mutant retained the ability to hydrolyze nitrocefin and gave a similar value as observed for WT BlaC ($4.2 \pm 0.3 \times 10^5\ \mathrm{M^{-1}s^{-1}}$). A 20-fold decrease in catalytic efficiency was observed for ampicillin ($0.07 \pm 0.03 \times 10^5\ \mathrm{M^{-1}s^{-1}}$).

Similar experiments were performed with ceftazidime (Figure S2.3), giving a $k_{\mathrm{cat}}/K_{\mathrm{M}}$ of $0.23 \pm 0.07 \times 10^3\ \mathrm{M^{-1}s^{-1}}$ for WT BlaC (eq. 2.6 See materials and methods), also consistent with published values.[72] The hydrolysis reaction with ceftazidime by BlaC P167S was monitored for an extended period of 1 hour. The first 5 min of product formation are presented in Figure S2.4, showing biphasic kinetics, with an initial burst followed by a linear phase. The amplitude of the burst phase (0.8 μM) was close to the enzyme concentration (1.0 μM). To determine whether the first phase of the curve represents a true burst, i.e. formation of the product linked to the enzyme, or is evidence of branched kinetics, as reported for several β-lactamases with bulky β-lactam antibiotic substrates,[145,146] ceftazidime hydrolysis by 100 nM BlaC P167S

was measured at different substrate concentrations (Figure 2.1), and the data were fitted to eq. 2.7 (See materials and methods), an empirical, model-agnostic formula that yields an initial and final velocity and a time constant for the conversion from phase 1 to phase 2.[147] The amplitude of the burst phase is dependent on the substrate concentration and greatly exceeds the enzyme concentration for high concentrations of ceftazidime (Table S2.2), indicating that the biphasic kinetics are a consequence of a branched kinetic pathway. The $k_{\mathrm{cat}}/K_{\mathrm{M}}$ of BlaC P167S with ceftazidime is 6.1 ± 0.8 × 10^3 $M^{-1}s^{-1}$ in kinetic phase 1. Determination of the K_{M} was not possible, indicating it is high, probably due to steric hindrance in the active site caused by the bulky side chains of ceftazidime.[133]

Thus, conversion of ceftazidime is much more efficient for the mutant than the WT enzyme, at least in the initial phase. The velocity of the second phase is nearly independent of the substrate concentration, which indicates that the apparent K_{M} of this phase is low. It can be estimated to be 1.2 ± 0.4 μM. For linear kinetics involving a covalent intermediate (eq. 2.1), the apparent K_{M} is defined by eq. 2.2, showing that the standard K_{M} is modified by the ratio of k_c and (k_b + k_c). Thus, it is concluded that the acylation rate constant (k_b) is much higher than the deacylation rate constant (k_c), yielding a low apparent K_{M}.

$$E + S \underset{k_{-\mathrm{a}}}{\overset{k_{\mathrm{a}}}{\rightleftharpoons}} ES \overset{k_{\mathrm{b}}}{\rightarrow} EI \overset{k_{\mathrm{c}}}{\rightarrow} E + P \tag{2.1}$$

$$K_{\mathrm{M}}^{\mathrm{app}} = \frac{k_{\mathrm{c}}}{k_{\mathrm{b}}+k_{\mathrm{c}}} \cdot \frac{k_{-\mathrm{a}}+k_{\mathrm{b}}}{k_{\mathrm{a}}} \tag{2.2}$$

$$k_{\mathrm{cat}} = \frac{k_{\mathrm{b}} \cdot k_{\mathrm{c}}}{k_{\mathrm{b}}+k_{\mathrm{c}}} \tag{2.3}$$

The branched pathway kinetics could be triggered by the chemical rearrangement of the acyl moiety or by an enzyme conformational change.[108,145] Such an isomerization of the resting state enzyme has also been described previously for a class C β-lactamase.[148] Therefore, to further clarify the possible kinetic mechanism for ceftazidime hydrolysis by BlaC P167S, NMR spectroscopy experiments were performed.

Table 1. Kinetic parameters for ampicillin, nitrocefin and ceftazidime hydrolysis by BlaC WT and P167S at 25 °C. The errors are the standard deviation over three experiments.

Substrate	Parameters	BlaC variants		
		Wildtype (WT)	P167S first phase	P167S second phase
Ampicillin (NaPi, 100 mM, pH 6.4.)	k_{cat} (s^{-1})	18 ± 2	0.1 ± 0.06	n/a[a]
	K_M^{app}(μM)	144 ± 18	12 ± 5	n/a
	k_{cat}/K_M^{app} (10^5 M^{-1} s^{-1})	1.3 ± 0.1	0.07 ± 0.03	n/a
Nitrocefin (NaPi, 100 mM, pH 6.4.)	k_{cat} (s^{-1})	120 ± 8	59.1± 0.7	n/a[a]
	K_M^{app}(μM)	215 ± 19	142 ± 10	n/a
	k_{cat}/K_M^{app} (10^5 M^{-1} s^{-1})	5.6 ± 0.6	4.2 ± 0.3	n/a
Ceftazidime (NaPi, 100 mM, pH 6.4.)	k_{cat} (s^{-1})	ND[b]	ND	0.005 ± 0.001
	K_M^{app}(μM)	ND	ND	1.2 ± 0.4
	k_{cat}/K_M^{app}(10^3 M^{-1} s^{-1})	0.23 ± 0.07	6.1 ± 0.8	4 ± 2
Ceftazidime (MES, 100 mM, pH 6.4.)	k_{cat} (s^{-1})	ND	ND	0.0065 ± 0.0005
	K_M^{app} (μM)	ND	ND	11 ± 2
	k_{cat}/K_M^{app}(10^3 M^{-1} s^{-1})	ND	1.3 ± 0.5	0.57 ±0.04

[a] n/a, not applicable

[b] ND, not determined

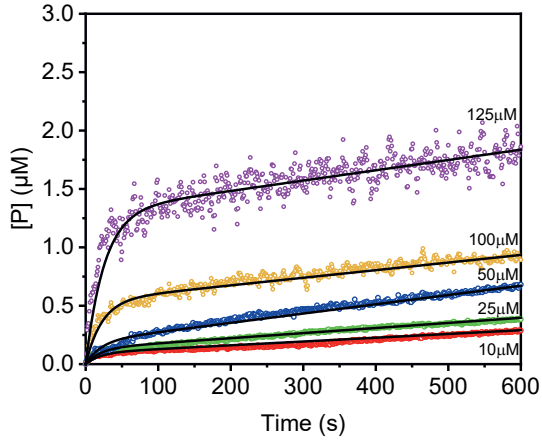

Figure 2.1 Biphasic kinetics of ceftazidime hydrolysis by BlaC P167S. Product curves of ceftazidime hydrolysis by BlaC P167S in phosphate buffer at various substrate concentrations are shown. The black line is the fit for the biphasic kinetics described by eq. 2.7, the fitting parameters are listed in Table S2.2.

BlaC P167S exists in two conformations.

To establish whether BlaC P167S can exist in more than a single conformation, ^{1}H-^{15}N TROSY-HSQC spectra were recorded before and during ceftazidime hydrolysis for 6 hours, until hydrolysis was complete. The spectra represent predominantly the second kinetic phase, because the first phase is completed in the first minutes. The NMR data revealed that BlaC P167S exists in two conformations in the absence of substrate, because the resonances for many residues gave two distinct signals. Interestingly, the first spectrum after addition of ceftazidime, recorded after 39 min, shows only one conformation of the enzyme and the second conformation is not observed until substrate hydrolysis is almost complete at around 6 hours (Figure 2a). To aid in distinguishing the two conformations, we define the conformation for which the resonances disappeared during the reaction as the open form and the other as the closed form, for reasons explained later. The closed form of the BlaC P167S mutant shows resonance positions more similar to those of the WT enzyme, suggesting the structures are more alike. The changes in the relative intensities of the two conformations during the hydrolysis process are shown in Figure 2b. The population of the open form was initially 50%. This form was completely depleted during the reaction and recovers to 25% after 743 min, whereas the population of the closed form is approximately 40% at this endpoint. One possible reason why the resonance intensities do not recover to their initial values when hydrolysis is complete is that association and dissociation of the high amount of product could cause chemical exchange broadening. It is also possible that at the end of the reaction part of the enzyme is lost due to aggregation. The presence of the large amount of product, which can associate with the protein, may also affect the ratio of the two forms, causing the lower fraction of the open form.

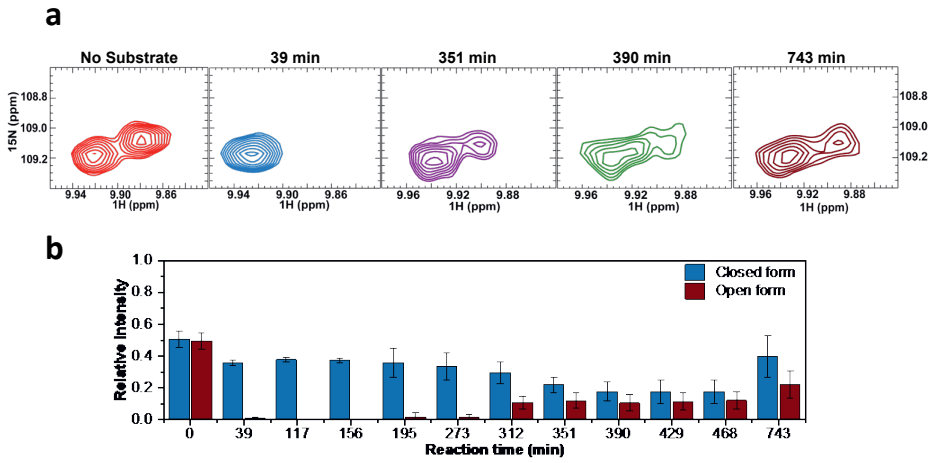

Figure 2.2 Two conformations of BlaC P167S. **a)** Detail of ^{1}H-^{15}N TROSY-HSQC spectra during ceftazidime hydrolysis, showing the double resonance for Gly120; **b)** Relative intensities of the two conformations (averaged over 15 residues: Thr98, Asp100, Gln114, Met117, Gly120, Asp124, Tyr151, Thr188, Lys203, Thr208, Arg222, Ala248, Ser265, Gly270, and Ala274) before, during and after ceftazidime hydrolysis. The data at 0 min represent the spectra without substrate. Error bars represent the standard deviation over 15 residues.

The Ω-loop of BlaC P167S is dynamic.

To structurally characterize the two conformations in the absence of substrate, the ^{1}H-^{15}N resonances of BlaC P167S were assigned by comparison to WT BlaC assignments and confirmed using HNCA and HNCACB spectra, obtained with a ^{13}C-^{15}N uniformly labelled sample. Phosphate can bind to specific residues in the active site of BlaC,[149] so the spectra were recorded in both MES and phosphate (NaPi) buffers at 20 °C. All non-proline backbone amides peaks were assigned except Asp2 and four residues in the active site, as in WT BlaC.[149] BlaC P167S exhibited two conformations in both MES and NaPi (Figure 2.3a and S2.5). The split peaks relating to these two conformations have a minimum distance of ~13-20 Hz for both ^{1}H and ^{15}N dimensions, evidence for slow chemical exchange (k_{ex} << 58 s^{-1}). The relative intensities of the split peaks indicate that the relative populations of the two states are 49% and 51% in NaPi, and 76% and 24% in MES buffer (Figure 2.3a). Spectra were also measured at 25 °C (Figure S2.6) and assigned on the basis of the spectra taken at 20 °C (Figure S2.5). The relative populations of the two states are 48% and 52%

in NaPi, and 71% and 29% in MES, indicating temperature has only a minor impact on the relative populations of the two states.

The relative intensities of the resonances in NaPi buffer for WT and P167S BlaC were plotted and found to match for some parts of the protein (e.g., up to residue 66, Figure 2.3c). For the part of the protein for which residues show double peaks, the sum of the two intensities is close to that of the same residue in the spectrum of WT BlaC (e.g., residues 150 - 163, Figure 2.3c). In some regions the intensities of mutant resonances were only about 40% of WT intensity, suggesting that these residues exist in two conformations but the resonance of the second conformation could not be detected, such as for Ω-loop and active site residues (Figure 2.3c). This observation suggests these resonances experience exchange broadening in one of the two conformations.

The chemical shift perturbations (CSPs) of the two conformations in NaPi buffer at 25 °C in comparison with the WT BlaC resonance positions were subsequently determined (Figure S2.7). Large CSPs were observed near Ile105 and Asp136 for both conformations. Major CSPs were observed in the Ω-loop around the mutation site and minor perturbations were found for residues that are distant from the mutation site. These CSPs indicate that the conformation of both open and closed forms of the enzyme differ from that of WT BlaC. The CSPs are, however, more extensive and larger for the open form (Figure S2.7).

Residues Pro167 – Arg171 of the Ω-loop are in an α-helical conformation in the WT enzyme (PDB ID: 2GDN). As large CSPs were observed in this region for BlaC P167S, we determined whether this α-helix remains present using the TALOS+ server,[150] which estimates the ϕ and ψ backbone torsion angles, via the backbone ^{13}C, ^{15}N and ^{1}H chemical shifts (Table S2.3). Residues Ser167 to Leu169 in the open state were predicted to be in an α-helical conformation based on the probability value from the server (Figure 2.3b). Random-coil-index-derived order-parameters (RCI-S^2)[151] of approximately 0.9 were obtained, indicating that the secondary structure of the predicted residues is rigid on the nanosecond time scale. The signals of the equivalent residues of the closed state were not observed (Figure 2.3c).

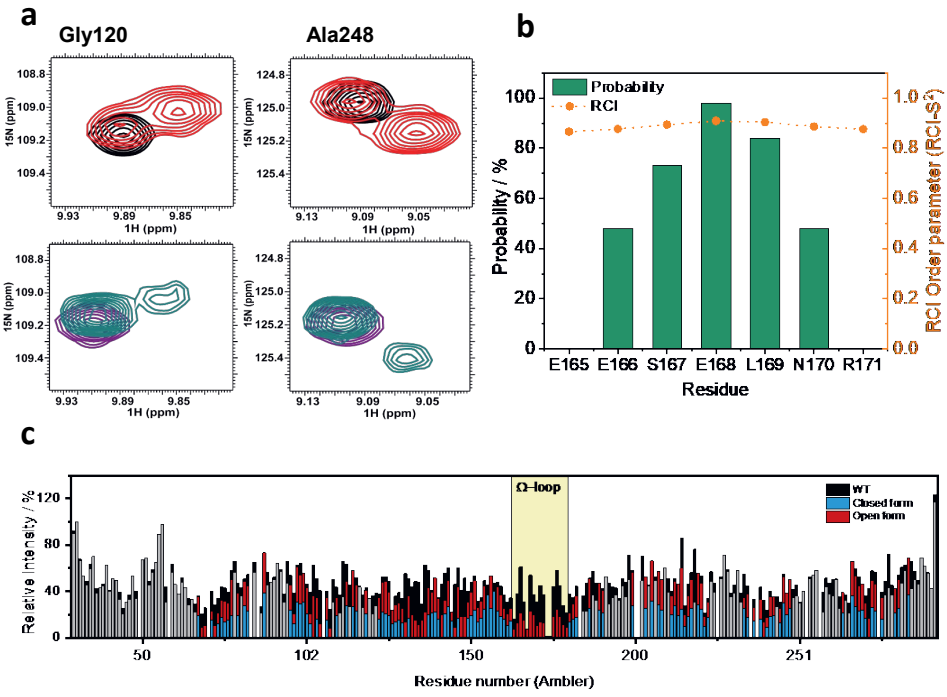

Figure 2.3 NMR spectra of BlaC P167S and the relative intensity plot. **a)** Detail of ^{1}H-^{15}N TROSY-HSQC spectra showing resonances for residues Gly120 (left) and Ala248 (right) of BlaC P167S in NaPi (red) and MES (teal) compared with WT in NaPi (black) and MES (purple) at 20 °C. Full spectra are shown in Figure S2.5; **b)** TALOS+ secondary structure prediction of Ω-loop residues (E165 to R171). Probabilities are shown as green bars and the random-coil-index-derived order-parameters (RCI-S^2) are represented by orange circles. Input data are listed in Table S3; **c)** Relative intensities of the open form (red) and closed form (blue) of BlaC P167S compared with WT (black). Grey bars represent peaks with only one resonance observed in the spectrum of BlaC P167S, with a relative intensity close to WT BlaC.

Phosphate binding increases the population of the open conformation.

We wondered why the relative populations of the two conformations of BlaC P167S are different in MES and NaPi buffer. Previous reports have noted that phosphate can bind to the carboxylate binding pocket in the active site,[149,152] which may affect the populations of the two observed conformations. To probe the effect of phosphate on the two conformations of BlaC P167S, TROSY-HSQC spectra were recorded at phosphate concentrations ranging from 0 to 250 mM and separately, with increasing

MES buffer concentrations as a control (Figure S2.8a). Resonances of residues in the phosphate binding sites shift with increasing phosphate concentration, indicating that binding happens in the fast-exchange regime. The residues that exhibit the largest CSPs match those described previously.[149] CSPs were observed for both conformers and the dissociation constants (K_{D1}, K_{D2}) were determined, yielding 60 ± 6 mM and 10 ± 3 mM for the closed and open forms, respectively (Figure 2.4b). Thus, phosphate binding is preferential in the open form, shifting the population equilibrium to this form (Figure 2.4a and S2.8b). The ratio of populations was not affected by increasing MES buffer concentration (Figure S2.8b). The equilibrium between the two conformations and binding/dissociation of phosphate can be represented in a thermodynamic square (Figure 2.4c), which can be used to show that the six-fold difference in dissociation constant can explain the observed change in the ratios of open and closed states (Figure 2.4d). The simulation yields equilibrium constants of 0.41 and 2.43 for the closed/open equilibrium in the absence and presence of phosphate, respectively.

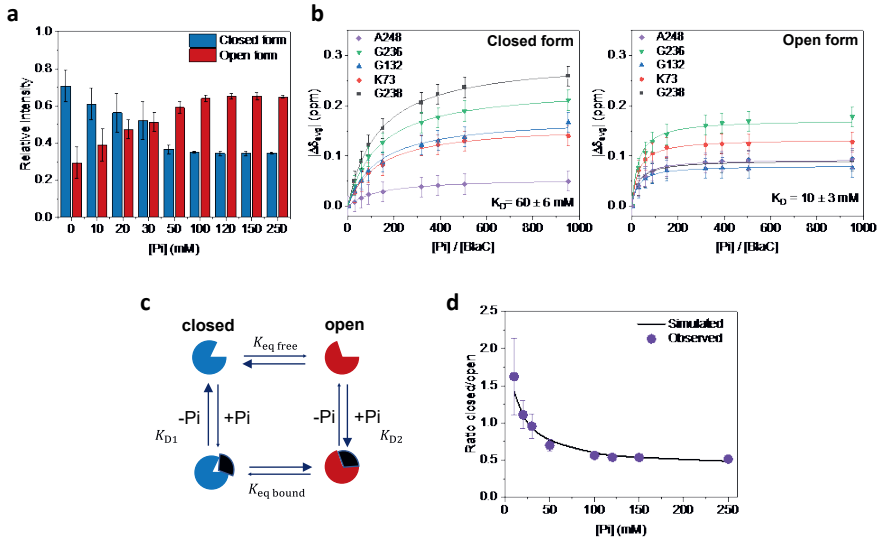

Figure 2.4 Phosphate effect on the open and closed forms of BlaC P167S at 25 °C. **a)** Relative intensity of the closed (blue) and open (red) conformations plotted as a function of phosphate concentration. Intensities were averaged over 55 residues. The errors are the standard deviation over duplicate measurements; **b)** CSP binding curves (eqs. 2.8 and 2.9). The estimated peak picking error (± 0.02 ppm) is shown as vertical error bars. The error in the K_D

is the fitting error; **c)** Thermodynamic square for phosphate binding to two conformers of BlaC P167S; **d)** The observed ratio of closed and open conformers (purple circles) is plotted as a function of the phosphate concentration. The errors are the standard deviation over duplicate measurements. The simulation assuming a 6-fold difference in affinity for phosphate between closed and open states is shown as a black line.

The crystal structure of BlaC P167S shows both conformations.

To visualize the conformational changes between the closed and open forms, a crystal structure of BlaC P167S was obtained. The protein crystallized at 1.8 Å resolution in the space group P1 with two molecules in the asymmetric unit, showing different conformations (Figure 2.5a). These conformations were observed in two crystals, which crystallized under different conditions (Table S2.4). The overall structure of the two conformations resembles the WT. However, a marked difference between the two conformations and the WT is observed within the Ω-loop, specifically from residues 164 to 177 (Figure 2.5). The likely reason for the changes is that the *cis* peptide bond between Glu166 and Pro167 changes into a *trans* bond upon mutation to Ser167 (Figure 2.5b). In one of the conformations the Ω-loop opens and expands the active site pocket. Such a phenomenon has been observed before to a lesser extent for TEM and CTX-M-9 β-lactamases.[135] TEM shows an increased ceftazidime resistance due to a conformational change in the Ω-loop.[133] Two Ω-loop states were also recently described in TEM variants that exhibit increased benzylpenicillin resistance, related to a higher population of open Ω-loop pockets.[95,140] However, no open Ω-loop pocket was found in WT BlaC.[95] Conformational change in the Ω-loop gives ceftazidime better access to the active site.[113,128,129] As a consequence of this repositioned Ω-loop, Glu166 is flipped to the outside of the enzyme and is consequently located far away from the active site. A possible stabilization of this conformation occurs via intermolecular crystal packing interactions (Figure S2.9). We named this conformer the open state. In contrast, the other conformation shows a (semi-)closed Ω-loop, which is more similar to the WT BlaC. This conformation appears to be stabilized by a hydrogen bond between the nitrogen atom of Ser104 and the OE1 atom of Glu168 and a salt bridge between Glu 165 and Arg103 (Figure. 2.5b). To enable this interaction, the peptide bond between Arg103 and Ser104 is flipped relative to the structure of wild type BlaC. The position of Glu166 in this

conformation is similar to that in the structure of the WT enzyme, although the carboxy group is rotated. B-factors of protein crystal structures reflect the fluctuation of atoms and provide insight into protein dynamics.[153] In the structures of BlaC P167S, the average observed B-factors within the Ω-loop of open state and closed state are 50.44 and 35.43 $Å^2$, respectively, whereas in WT BlaC it is 17.17 $Å^2$ (Figure 2.5c). Thus, the Ω-loop is more dynamic in the mutant in both forms. Interestingly, the neighboring regions, which show some flexibility in WT BlaC, are more restrained in the mutant.

In the open conformation, the Ω-loop contains an α-helix in the crystal structure, in accordance with the helix observed for one of the conformations in solution, as supported by the TALOS+ analysis (Figure 2.3b). This α-helix is not observed in the closed conformation of the Ω-loop. Therefore, we assigned the conformation with an α-helix in the Ω-loop in solution to the open conformation in the crystal.

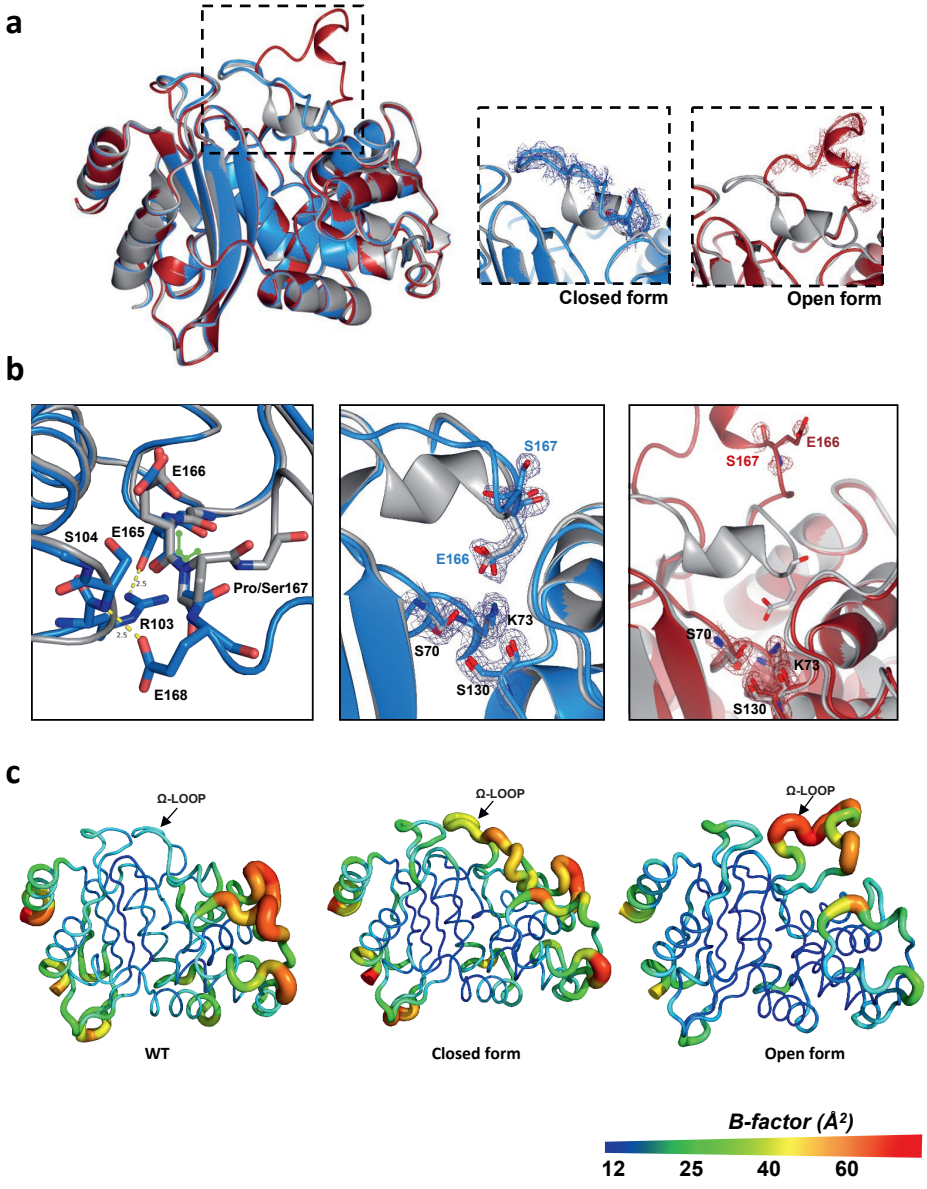

Figure 2.5 Crystal structure of the open and closed forms of BlaC P167S. **a)** X-ray crystal structure of the resting state of BlaC P167S. The open form is shown in red, and the closed form in blue; both forms are shown overlaid with the WT BlaC structure (grey, PDB 2GDN[72]) for reference. The images on the right show a close-up of the Ω-loop. The residue shown in sticks is Ser167; **b)** The positions of Arg103, Ser104, Ser167, Glu165, Glu168, Glu166,

Ser130, Lys73, Ser167, and Ser70 in the active site. Potential hydrogen bonds between Arg103 and Glu165 as well as Ser104 and Glu168 are shown as a yellow dashed line. Atom distances are indicated in Å. The green bar indicates the *cis* peptide bond in Pro167. Colors are the same as in panel (a). The $2mF_0$-DF_c electron density map is centered on the Ω-loop and selected active site residues and is shown in blue chicken wire for the closed form and brown for the open form, with a contour level of 1 σ and extent radius of 5 Å. **c)** Backbone B-factors of BlaC WT and the closed and open forms of BlaC P167S. Heat colors and thicknesses of the tubes correlate with B-factors. The Figure was produced using PYMOL.[154] The B-factors range from 12.9 $Å^2$ to 67.8 $Å^2$.

A branched kinetics model for ceftazidime hydrolysis.

Our data indicate that the BlaC P167S mutant possesses two conformations in the resting state. Crystal structures of two conformations (open vs. closed) of P167S were solved, and these structures are supported by the NMR spectra. To explain the biphasic kinetics for ceftazidime hydrolysis, we propose that the conformations can slowly interconvert, which is supported by the changing population ratio upon titration with phosphate. This interconversion leads to a branched kinetic model, which in its simplest form only shows interconversion for the resting state conformations (Figure 2.6a), although interconversion during the catalytic cycle cannot be ruled out.

To test this model, the kinetic data for ceftazidime hydrolysis in MES buffer were simulated by numerically solving the differential equations describing the model in Figure 2.6a. The data can be simulated reasonably well (Figure 2.6b, Figure S2.10) with the parameters shown in Table S2.5. These parameters show that the closed form (E_1) has an 800-fold lower deacylation rate constant than the open form (E_2) ($k_4 \ll k_{12}$), so the acyl intermediate formed by the closed form (E_1I, species D) accumulates and is the major form present during hydrolysis, an observation that is consistent with loss of the signals from the open form in the real-time NMR data. The acylation rate of the closed form is much higher than the deacylation rate ($k_3 \gg k_4$), leading to a strongly reduced apparent K_M (eq. 2.4), in line with observations for the second-phase kinetics.

$$\boldsymbol{K_M^{app} = \frac{k_4 \cdot k_5}{k_3 \cdot k_4 + k_4 \cdot k_5 + k_3 \cdot k_5} \cdot \frac{k_2 + k_3}{k_1}} \qquad (\mathbf{2.4})$$

The higher deacylation rate of the open form explains the high reaction rate in the first phase of the kinetics. The slow interconversion between open and closed states (k_7 and k_8), in combination with the accumulation of E_1D is the reason for the conversion from the fast to the slow phase of the kinetics. The exchange rate constant ($k_7 + k_8$) is 3.0 min^{-1} according to the simulation, in line with the value obtained with the fit to eq. 2.3 (2.8 min^{-1}) and indeed much lower than the upper limit set by the NMR data (<< 57 s^{-1}). It is noted that even the minimal model shown in Figure 2.6a contains many parameters and it is expected that parameters may correlate, and other values may also give acceptable results. Thus, the presented values should be treated with caution and the simulation merely serves to show that the model is able to explain all observations.

The reason for the low deacylation rate in the closed state remains unclear. The activity in the open state indicates that Glu166 is not required, because it is located far from the active site. The mechanism for deacylation of the ceftazidime adduct is therefore unclear. The active site residue Lys73 has been proposed to take the role of Glu166.[155] It has also been suggested that it could be dependent on the conformation of the adduct,[156] therefore it is possible that the closed state hinders the adduct in assuming the right conformation. The loss in activity of BlaC P167S compared to WT BlaC for ampicillin is much larger than for nitrocefin and the data suggest that slow hydrolysis of the former is due a low deacylation rate because of the low apparent K_M. It has been hypothesized that a larger active site cavity would not make optimal contacts with smaller antibiotics, making it less effective for catalysis.[157] For hydrolysis of the ampicillin and nitrocefin adducts, Glu166 is essential and it is likely that changes in the omega loop due to the P167S mutation affect the structure and dynamics, and thus the ability of Glu166 to activate the active site water molecule. Finetuning of the active site around Glu166 may be critical in determining the deacylation capability of the adducts of these and other substrates.

Conclusions

The mutation P167S changes the structure of the Ω-loop in BlaC, resulting in two

conformations for the resting state of the enzyme, both in the crystalline state and in solution. One state is (semi-)closed whereas the other exposes a large part of the Ω-loop to the solution. The open state is most active against ceftazidime. The (semi)closed form has a slow deacylation reaction, and consequently this state accumulates under steady state conditions. The turnover rate of ampicillin is compromised by the P167S mutation. The difference in the catalytic mechanisms, i.e. whether Glu166 is required, underlies the trade-off in activities seen for β-lactamases in the conversion of penicillins and ceftazidime. Though all these substrates have a β-lactam group, they require a different mechanism to catalyze hydrolysis.

a

$$E_1(A) + S(B) \underset{k_2}{\overset{k_1}{\rightleftharpoons}} E_1S\ (C) \overset{k_3}{\rightharpoonup} E_1I\ (D) \overset{k_4}{\rightharpoonup} E_1P(E) \underset{k_6}{\overset{k_5}{\rightleftharpoons}} E_1(A) + P(F)$$

$$k_7 \downarrow\uparrow k_8$$

$$E_2(G) + S(B) \underset{k_{10}}{\overset{k_9}{\rightleftharpoons}} E_2S\ (H) \overset{k_{11}}{\rightharpoonup} E_2I\ (I) \overset{k_{12}}{\rightharpoonup} E_2P(J) \underset{k_{14}}{\overset{k_{13}}{\rightleftharpoons}} E_2(G) + P(F)$$

b

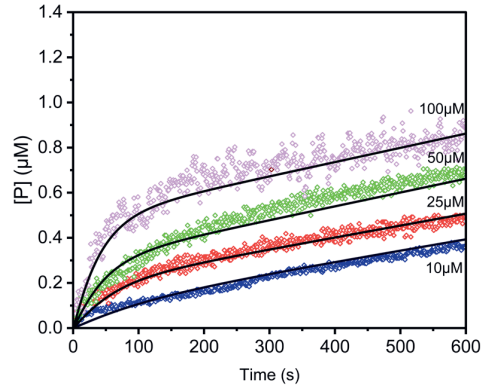

Figure 2.6 An overall framework for ceftazidime hydrolysis with BlaC P167S. **a)** Scheme for the kinetic mechanism of BlaC P167S hydrolysis with ceftazidime. **b**) Progress curves of ceftazidime hydrolysis by BlaC P167S as a function of substrate concentration. The black line is the simulated data by the proposed scheme for the kinetic mechanism (Figure 2.6a) with the parameters in Table S2.5.

Materials and Methods

Laboratory evolution

Error-prone polymerase chain reactions (EP-PCR) were performed using an *E. coli* expression-optimized *blaC* gene (amino acid sequence in Fig S11). DreamTaq DNA Polymerase (0.1 U/µL, Thermo Scientific) was used with manganese chloride (0.2 mM $MnCl_2$), magnesium chloride (2 mM $MgCl_2$), dATP/dGTP (0.2 mM) and dCTP/dTTP (0.52 mM) to increase the error rate. The mutated *blaC* genes were cloned behind the *lac* promotor in pUK21 through restriction and ligation. *E. coli* KA797[158] cells were transformed with the plasmid library and plated on lysogeny broth (LB) agar plates with kanamycin (50 µg/mL), isopropyl β-d-1-thiogalactopyranoside (IPTG, 1 mM), and ceftazidime (1 µg/mL). The plates were incubated at 23 °C, 30 °C or 37 °C, for 3 days, 18 hours and 12 hours respectively. Around 5×10^5 clones were screened at each temperature, and three *blaC* clones were found on the plate incubated at 30 °C. The colonies were transferred to LB liquid cultures and incubated overnight at 37 °C and 250 rpm. Plasmids were isolated and transformed into fresh KA797 cells to confirm that resistance was the result of mutations in the *blaC* gene and not due to changes of the host cell. The mutated *blaC* genes were sequenced and the individual mutations were created in the *blaC* gene by QuikChange site-directed mutagenesis (Agilent) and verified by DNA sequencing.

Antimicrobial susceptibility testing

Antibiotic resistance was tested in *E. coli* cells carrying pUK21-*blaC* plasmids[158] with the gene behind the *lac* promotor. Drops of 10 µL of *E. coli* KA797 cultures with optical densities (OD_{600}) of 0.3, 0.03, 0.003 and 0.0003 were applied on the LB plates containing 50 µg/mL kanamycin, 1 mM IPTG, and varying concentrations of antibiotics. The plates were incubated at 23 °C, 30 °C and 37 °C until growth was visible.

Protein production and purification

The genes for WT BlaC and the BlaC P167S were cloned into pET28a plasmids[158] downstream of an N-terminal His-tag and a TEV cleavage site (Figure S2.12) and

expressed in *E. coli* BL21 (DE3). The proteins were produced and purified according to previously described protocols.[149] Pure protein was stored at −80 °C in 100 mM sodium phosphate buffer (pH 6.4).

Circular dichroism

Circular dichroism spectra were obtained using a Jasco J-815 circular dichroism spectrometer fitted with a Peltier temperature controller (Jasco). Measurements were performed at 25 ˚C with 7 µM protein in 100 mM sodium phosphate buffer (pH 6.4) and recorded from 260 to 190 nm. Measurements were performed in triplicate using a 1 mm quartz cuvette and spectra were normalized according to protein concentration.

Thermal shift assay

The thermal stability of the proteins was analyzed with a thermal shift assay using a CFX96 Touch Real-time PCR Detection System (BioRad). The commercially available stock of SYPRO Orange dye has a 5000x concentration. Samples of 10 µM protein with 4x concentration of SYPRO Orange dye in 100 mM sodium phosphate buffer pH 6.4 (68.68 mM NaH_2PO_4 and 31.32 mM Na_2HPO_4, the ionic strength is about 164 mM) were measured by fluorescence over a temperature range from 10 to 90 ˚C in increments of 1˚C for 1 min. Melting temperatures were determined from the derivatives of the obtained curves. Errors were determined as the standard deviation of triplicate measurements.

Enzyme kinetics

In vitro kinetic parameters were determined by monitoring the absorption change at 486 nm for nitrocefin ($\Delta\varepsilon$ = 11300 $M^{-1}cm^{-1}$)[159], 235 nm for ampicillin ($\Delta\varepsilon$ = 861 $M^{-1}cm^{-1}$)[158], and 260 nm for ceftazidime ($\Delta\varepsilon = 7\ (\pm 1) \times 10^3$) $M^{-1}cm^{-1}$, determined in this work and in line with previously reported values)[107,160], using a thermostatted PerkinElmer Lambda 1050+ UV-Vis spectrometer. All kinetic measurements were performed in triplicate at 25 ˚C. Ampicillin hydrolysis was measured at various concentrations in 100 mM sodium phosphate buffer (pH 6.4) with 20 nM WT BlaC or 200 nM BlaC P167S for a duration of 5 min. Nitrocefin conversion by 2 nM WT

BlaC or P167S was followed for 3 min. OriginPro (OriginLab) was used to fit initial velocities to the Michaelis-Menten equation eq. 2.5:

$$v_{\mathrm{i}} = \frac{k_{\mathrm{cat}}[E][S]}{K_{\mathrm{M}}+[S]} \tag{2.5}$$

Where v_i is the initial velocity, [E] and [S] are the enzyme and substrate concentrations, respectively. For ceftazidime hydrolysis, substrate was added to 0.1 or 1 μM WT BlaC or BlaC P167S in 100 mM sodium phosphate buffer (pH 6.4) or 100 mM MES buffer pH 6.4 (100 mM MES buffer pH 6.4 (100 mM MES hydrate and the NaOH is added to adjust pH to 6.4, the ionic strength is about 33 mM). Determination of V_{max} was not possible due to the high $K_{\mathrm{M}}^{\mathrm{app}}$ values, therefore eq. 2.6 was used, as the limiting case of eq. 2.5 ([S] << K_{M}), to determine the catalytic efficiency ($k_{\mathrm{cat}}/K_{\mathrm{M}}$):

$$v_{\mathrm{i}} = \frac{k_{\mathrm{cat}}}{K_{\mathrm{M}}}[E][S] \tag{2.6}$$

Two-phase kinetics was analyzed using eq. 2.7:[147]

$$P_{\mathrm{t}} = v_{\mathrm{s}}t - (v_{\mathrm{s}} - v_i)(1 - e^{-kt})/k \tag{2.7}$$

where P_{t} is the concentration of product at time t, v_i is the initial velocity and v_{s} is the velocity at steady state, and k is the apparent first-order rate constant for the progression from v_i to v_{s}.

Nuclear magnetic resonance (NMR) spectroscopy

Backbone assignments for 0.5 mM [^{15}N, ^{13}C] BlaC P167S were obtained with a set of standard HNCA, HNCACB, HNcaCO, HNCO, and TROSY-HSQC experiments that were recorded on a Bruker AVIII HD 850 MHz spectrometer with a TCI cryoprobe at 20 °C in 100 mM sodium phosphate buffer at pH 6.4, or 100 mM MES buffer (pH 6.4), with 1 mM TSP (trimethylsilylpropanoic acid) and 6% D_2O. Data were processed with Topspin 4.1.1 (Bruker Biopin) and analyzed using CCPNmr.[161]

TROSY-HSQC and HNCA spectra of wild-type BlaC[149] were used as a reference for the spectra of BlaC P167S (Biological Magnetic Resonance Bank [BMRB] accession no. 27067). The assignments for BlaC P167S have been deposited in the BMRB under access code (BMRB: 51876). The average chemical shift perturbations (CSPs), $\Delta\delta$, of the ^{1}H ($\Delta\delta_1$) and ^{15}N ($\Delta\delta_2$) resonances of backbone amides were calculated with eq. 2.8.

$$\Delta\delta = \sqrt{\frac{1}{2}\left[{\Delta\delta_1}^2 + \left(\frac{\Delta\delta_2}{5}\right)^2\right]} \tag{2.8}$$

Titrations of the [^{15}N] labeled BlaC P167S with sodium phosphate were done by measuring TROSY-HSQC spectra. As the buffer concentration increased from 10 mM to 250 mM, the protein concentration decreased from 350 to 262 µM. The association constant (K_A) of non-linear regression fitting was determined in OriginPro with eq. 2.9.[162]

$$CSP = 0.5\, CSP_{\max}(A - \sqrt{A^2 - 4R})$$
$$A = 1 + R + \frac{C_{\text{stock}} + E_{\text{i}}R}{C_{\text{Stock}}E_{\text{i}}K_{\text{A}}} \tag{2.9}$$

where $CSP_{\max}$ is the maximal chemical shift perturbation for selected residues, R is the molar ratio of phosphate and enzyme, C_{stock} is the concentration of phosphate stock (1 M) for the titration and E_{i} is the initial concentration of the enzyme. The phosphate titration experiments were performed in duplicate.

Real-time NMR measurements were performed by addition of ceftazidime (10 mM) to [^{15}N] labelled BlaC P167S (90 µM) and recording TROSY-HSQC spectra during catalysis every 39 min for 13 h at 25 °C. The sample contained 100 mM sodium phosphate buffer (pH 6.4), 1 mM TSP and 6% D_2O.

Protein crystallization

Crystallization conditions for BlaC P167S at a concentration of 10 mg mL $^{-1}$ were screened by the sitting-drop vapor diffusion method using the BCS, Morpheus, and

JCSG$^+$ (Molecular Dimensions) screens at 20 °C with 200 nL drops with a 1:1 protein:condition ratio.[163] Crystals for BlaC P167S grew within two weeks in 0.1 M sodium cacodylate (NaCacod) buffer, pH 6.29, with 1.02 M trisodium citrate (Na_3Cit) as precipitant. Two crystals from different wells were mounted on cryoloops in mother liquor, with the addition of 20% glycerol and flash frozen in liquid nitrogen for X-ray data collection.

Data collection and structure refinement

Data for the BlaC P167S variant structures were collected at the European Synchrotron Radiation Facility on the MASSIF beamline.[164] Data was obtained to 1.12 Å resolution. The diffraction data were indexed and integrated using XDS[165] and scaled using Aimless.[166] Due to anisotropy, the resolution was set to 1.8 Å and 1.9 Å, respectively, based on the resolution in the worst direction and the PDB entry 2GDN[72] served as the model for molecular replacement, which was performed with MOLREP[167] from the CCP4 suite.[167] Model building and refinement were performed in Coot and REFMAC.[167] The PDB-REDO Web server was used to further optimize and refine the model.[168] Two chains were obtained in the structure and the residues Thr55, Glu165, Val261, and Arg275 were modelled in two conformations. The duplicate structures of P167S have been deposited in the Protein Data Bank, accession codes (PDB: 8OE1 and 8OE5). The refinement and data collection statistics are given in the supplementary information (Table S2.4).

Supporting information

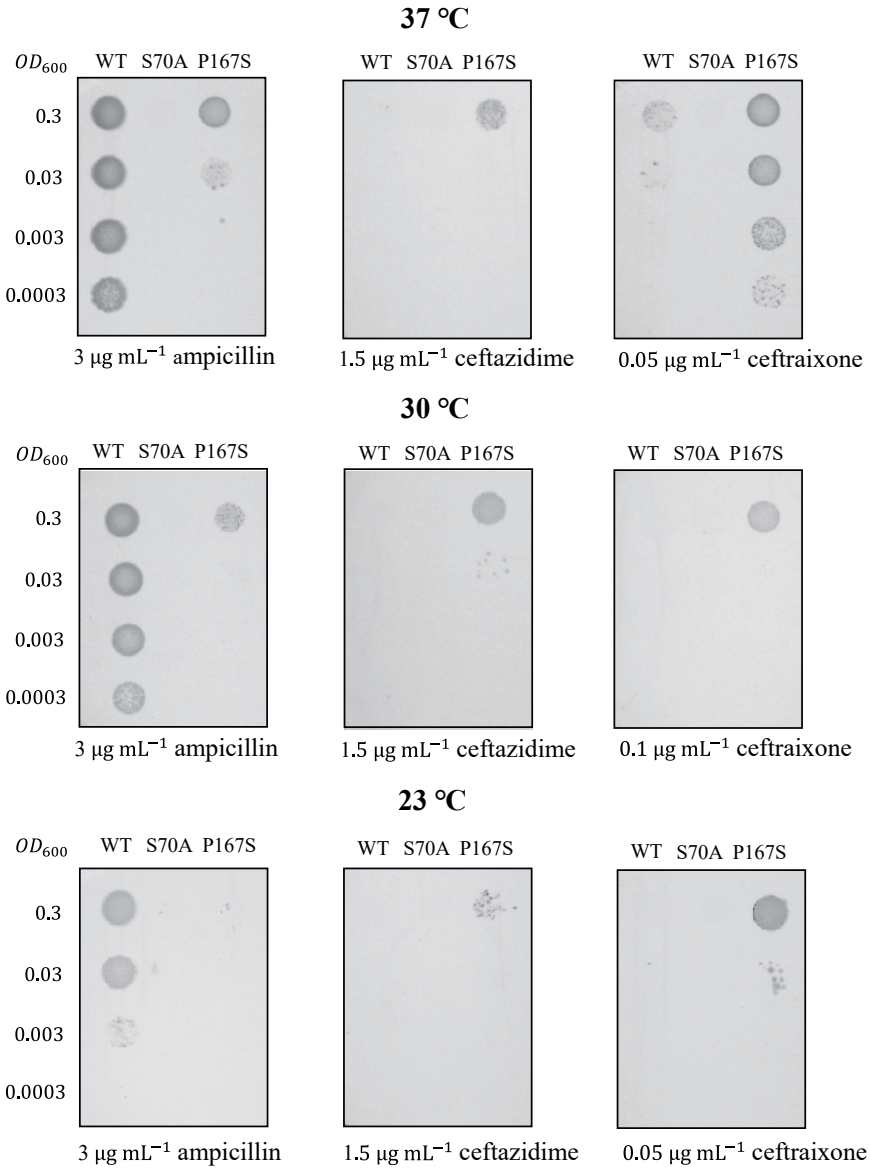

Figure S2.1 The activity of BlaC mutants in *E. coli* cells at 37 °C, 30 °C, and 23 °C with various concentrations of ampicillin, ceftazidime, and ceftriaxone. BlaC S70A, which cannot hydrolyze substrates is a negative control.

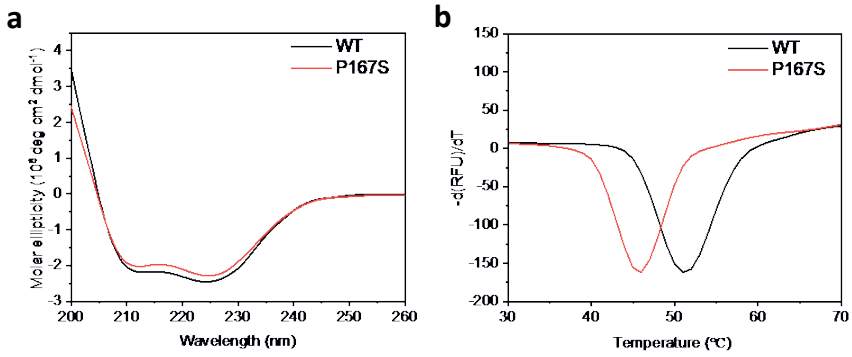

Figure S2.2 Secondary structure and thermostability of BlaC WT and P167S. **a**) Circular dichroism spectra and **b**) thermal shift assay (SYPRO orange binding) showing the normalized negative derivative of the fluorescence signal. The minimum in the curve defines the melting temperature (T_m).

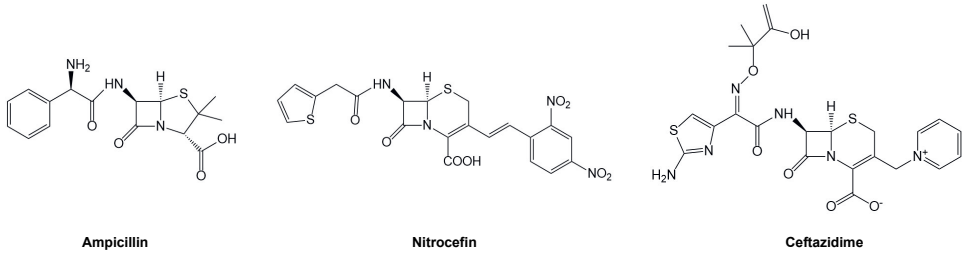

Figure S2.3 Chemical structures of ampicillin, nitrocefin, and ceftazidime.

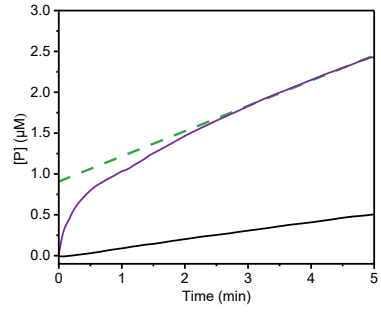

Figure S2.4 Ceftazidime hydrolysis. The first 5 min of ceftazidime hydrolysis (initial concentration of ceftazidime 25 μM) by WT BlaC (1 μM, black line) and BlaC P167S (1 μM, purple line) at 25 ˚C are shown. The concentration of the product (P) is plotted vertically. The dashed green line shows the tangent of the linear phase of the reaction catalyzed by BlaC

P167S and is extrapolated to estimate the amplitude of the burst phase.

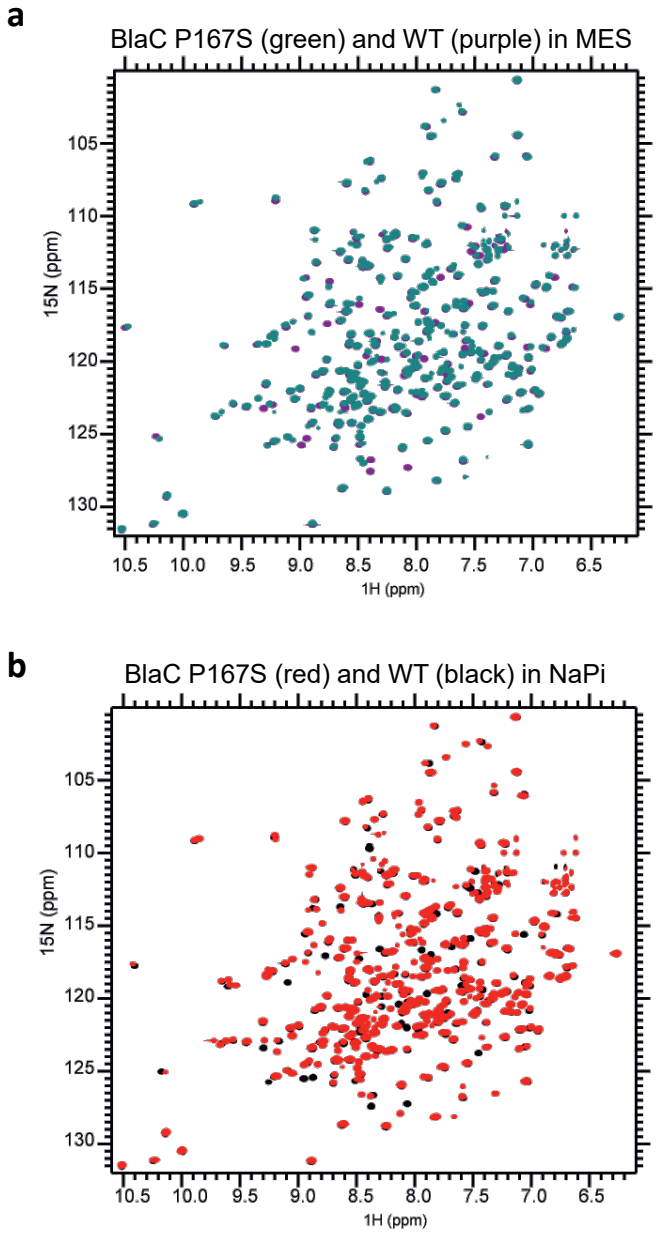

Figure S2.5 ^{1}H-^{15}N TROSY-HSQC spectra of BlaC P167S in different buffers at 20 °C. **a)** Overlay of BlaC P167S (teal) and WT (purple) in 100 mM MES buffer (pH 6.4); **b)** Overlay of BlaC P167S mutant (red) and WT (black) in 100 mM phosphate buffer (pH 6.4).

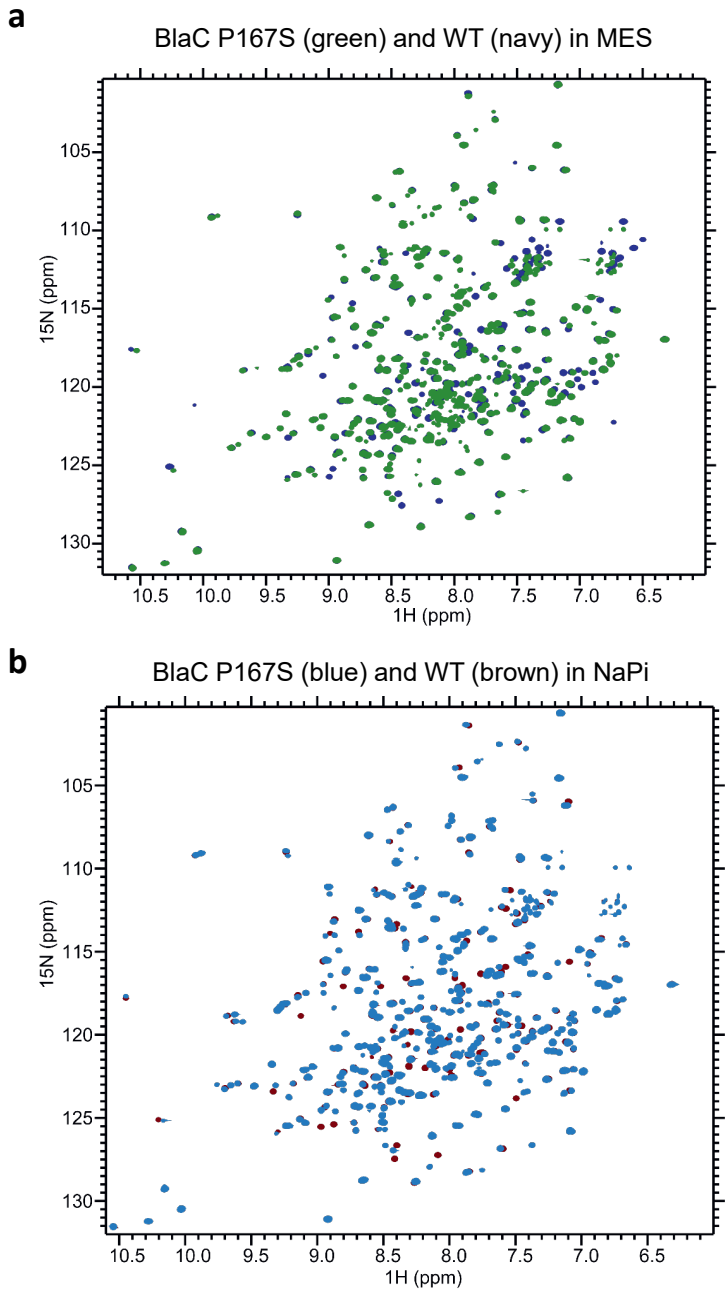

Figure S2.6 ^{1}H-^{15}N TROSY-HSQC spectra of BlaC P167S in different buffers at 25 °C. **a)** Overlay of BlaC P167S (green) and WT (navy) in 100 mM MES buffer (pH 6.4); **b)** Overlay of BlaC P167S (blue) and WT (brown) in 100 mM phosphate buffer (pH 6.4).

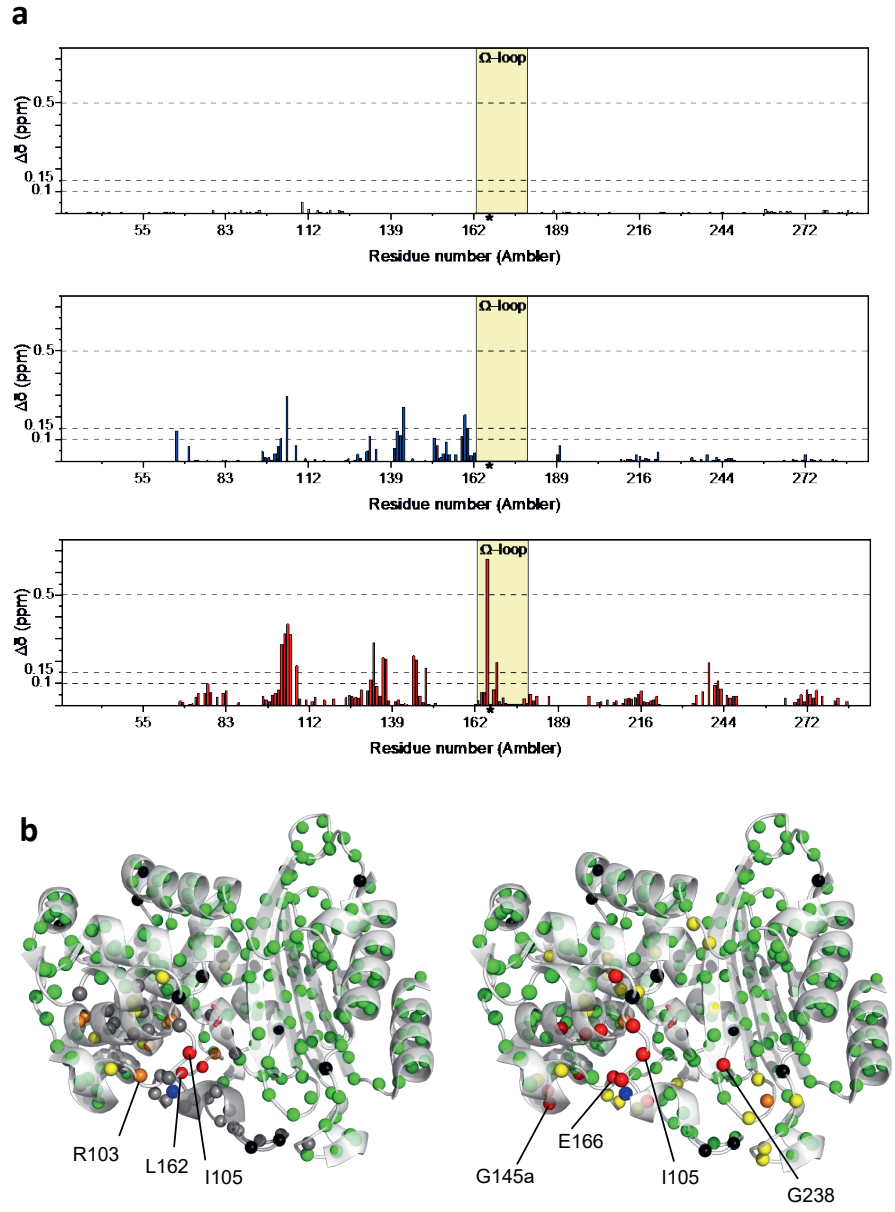

Figure S2.7 Average chemical shift perturbations (CSP) of BlaC P167S backbone amide resonances. **a)** Plot of average absolute CSP (compared with the WT chemical shifts using eq. 2.8, see Materials and Methods). The top panel (grey bars) gives the CSP for residues that show a single resonance with a relative intensity close to that of WT BlaC. The middle and

bottom panels show the CSP histograms for regions that represent the closed (blue bars) and open (red bars) forms; **b)** CSPs plotted on the structure of WT BlaC (PDB 2GDN) for the closed (left) and open (right) forms. Backbone amides are indicated as spheres. Yellow: 0.05 < CSP ⩽ 0.1 ppm, orange: 0.1 < CSP ⩽ 0.15 ppm, red: CSP > 0.15 ppm, green: CSP ⩽ 0.05 ppm, including data from top panel of (a). Grey: peaks that cannot be detected in the closed form. Black: no data available (proline or unassigned). Blue: mutation site Pro167.

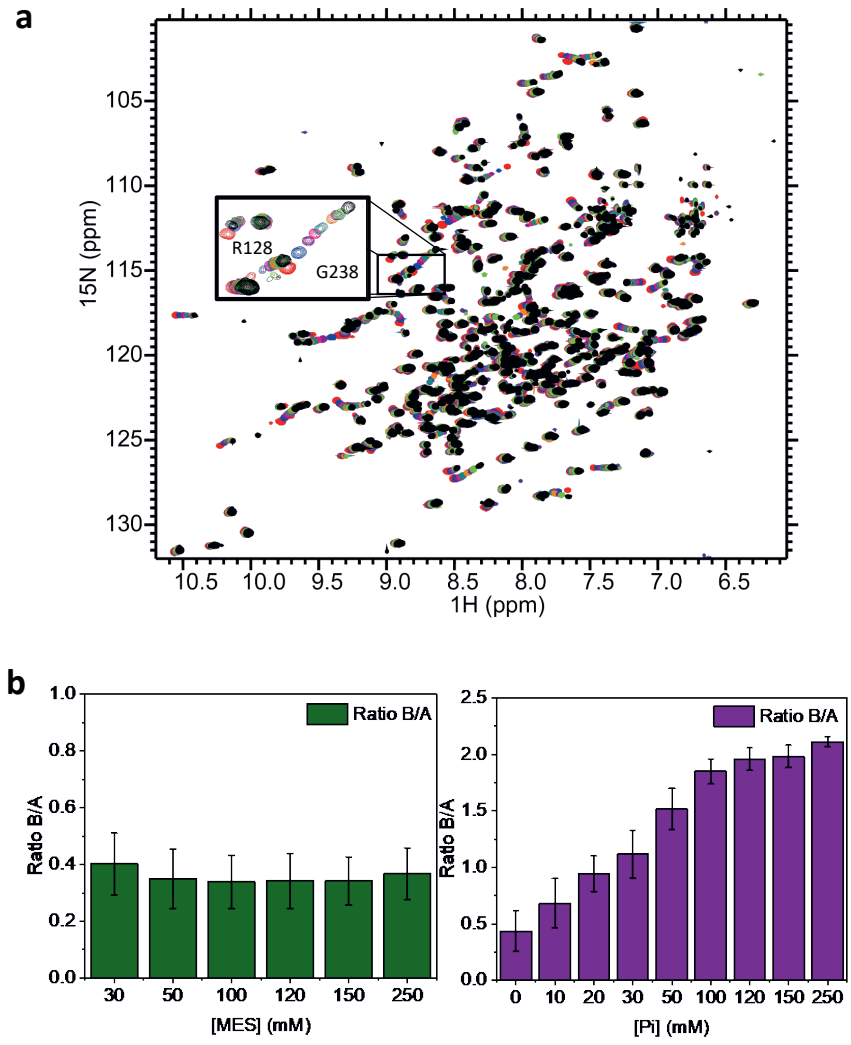

Figure S2.8 The effect of phosphate binding on the two conformations of BlaC P167S. **a)** Overlay of ^{1}H-^{15}N TROSY-HSQC spectra of BlaC P167S (350 µM) upon titration with phosphate. The sample contained 20 mM MES (pH 6.4) with 1 mM TSP and 6% D_2O, without (red peaks), and with 10 mM (blue), 20 mM (purple), 30 mM (pink), 50 mM (teal), 100 mM (orange), 120 mM (mauve), 150 mM (lime), 250 mM (black) sodium phosphate, respectively. Selected residue numbers are shown in the inset; **b)** Population ratio changes between open form (B) and closed form (A) as a function of buffer concentration. The ratios in MES (left)

are averaged over 36 residues. The ratios in NaPi (right) are averaged over 55 residues and the error is the standard deviation over duplicate titrations.

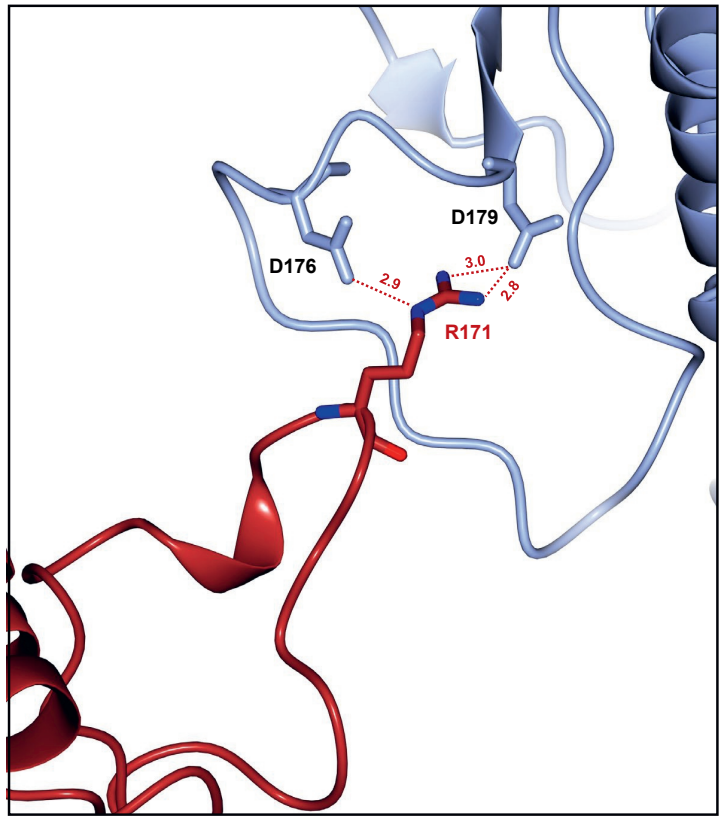

Figure S2.9 The open form of BlaC P167S is shown in red and the crystal symmetry mate is shown in pale blue. An interaction between Arg171 in one protein molecule and Asp176 and Asp179 in the other are shown. Atom distances are indicated in Å.

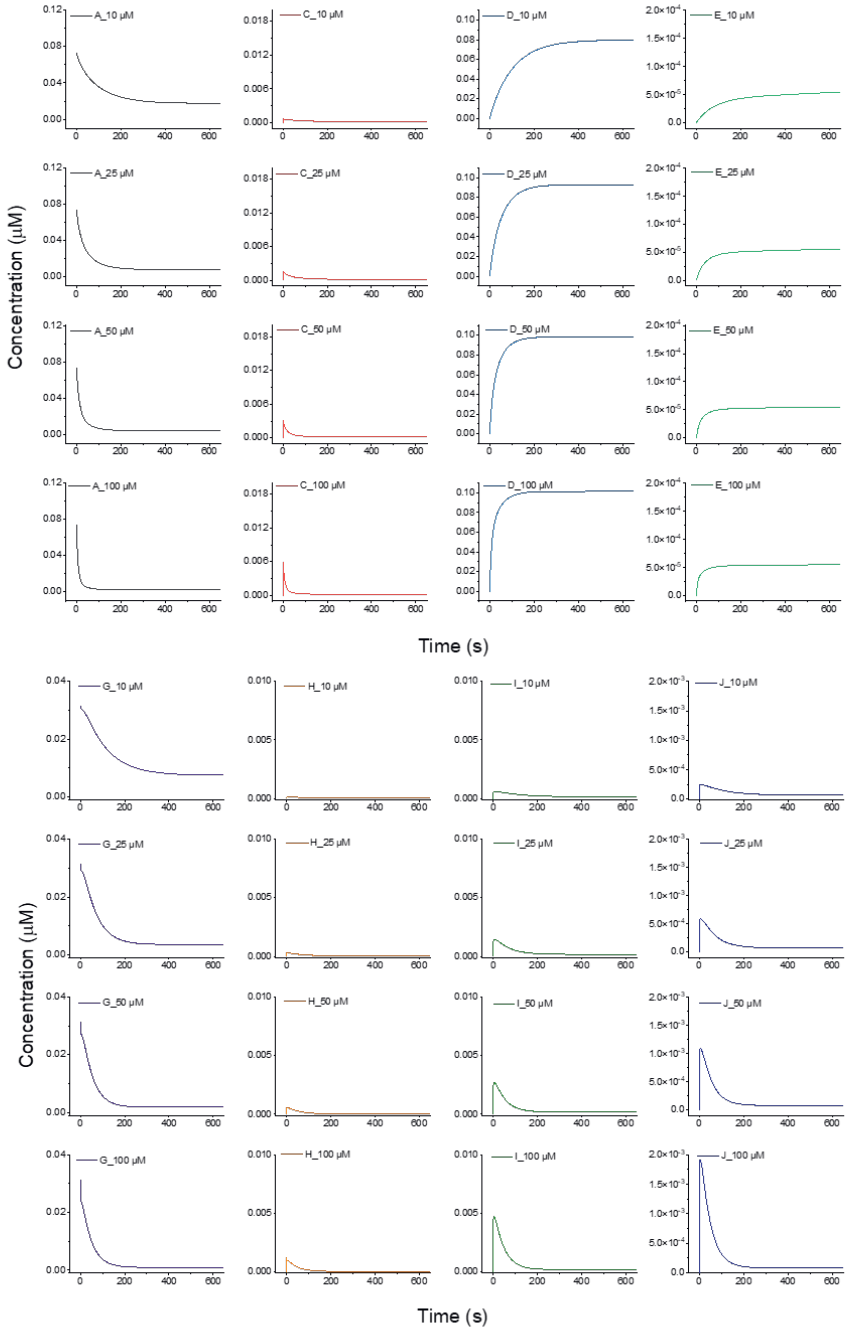
A_10 µM
C_10 µM
D_10 µM
E_10 µM
A_25 µM
C_25 µM
D_25 µM
E_25 µM
A_50 µM
C_50 µM
D_50 µM
E_50 µM
A_100 µM
C_100 µM
D_100 µM
E_100 µM
Concentration (µM)
Time (s)
G_10 µM
H_10 µM
I_10 µM
J_10 µM
G_25 µM
H_25 µM
I_25 µM
J_25 µM
G_50 µM
H_50 µM
I_50 µM
J_50 µM
G_100 µM
H_100 µM
I_100 µM
J_100 µM
Concentration (µM)
Time (s)

Figure S2.10 Ceftazidime hydrolysis of BlaC P167S mutant in 100 mM MES, pH 6.4 and the change of different species refers to the simulation model (Figure 2.6a) during the hydrolysis as a function of substrate concentration, where A represents the closed form (E_1) and G represents the open form (E_2), B is the substrate (S), F is product (P) and C, D, E, H, I, J represent E_1:S, E_2:S, E_1:I, E_2:I, E_1:P, and E_2:P.

```
                                                      30         40
MANNDLFQAS RRRFLAQLGG LTVAGMLGPS LLTPRRATAA QADLADRFAE LERRYDARLG

   50         60         70         80         90         101
VYVPATGTTA AIEYRADERF AFCSTFKAPL VAAVLHQNPL THLDKLITYT SDDIRSISPV

111        121        131        141            150        160
AQQHVQTGMT IGQLCDAAIR YSDGTAANLL LADLGGPGGG TAAFTGYLRS LGDTVSRLDA

   170        180        190        200        210        220
EEPELNRDPP GDERDTTTPH AIALVLQQLV LGNALPPDKR ALLTDWMARN TTGAKRIRAG

   230        240        250        260        270        280
FPADWKVIDK TGTGDYGRAN DIAVVWSPTG VPYVVAVMSD RAGGGYDAEP REALLAEAAT

 290
CVAGVLALEH HHHHH
```

Figure S2.11 The amino acid sequence of BlaC was used for *in vivo* experiments. Residues 28 -293 correspond to residue numbers 43-307 of the BlaC Uniprot sequence P9WKD3-1 and are numbered according to the Ambler notation. The TAT signal sequences are underlined, and the His-tag residues are highlighted in grey.

```
                                    30         40         50         60
MGSSHHHHHH SSGLVPRGSH MENLYFQGDL ADRFAELERR YDARLGVYVP ATGTTAAIEY

        70         80         90         101        111        121
RADERFAFCS TFKAPLVAAV LHQNPLTHLD KLITYTSDDI RSISPVAQQH VQTGMTIGQL

       132        142        148        158        168        178
CDAAIRYSDG TAANLLLADL GGPGGGTAAF TGYLRSLGDT VSRLDAEEPE LNRDPPGDER

       188        198        208        218        228        238
DTTTPHAIAL VLQQLVLGNA LPPDKRALLT DWMARNTTGA KRIRAGFPAD WKVIDKTGTG

       249        260        270        280        290
DYGRANDIAV VWSPTGVPYV VAVMSDRAGG GYDAEPREAL LAEAATCVAG VLA
```

Figure S2.12 The amino acid sequence of BlaC used for *in vitro* experiments. Residues of the TEV-cleavable His-tag are highlighted in grey. Residues 28-293 correspond to residue numbers 43-307 of the BlaC Uniprot sequence P9WKD3-1 and are numbered according to the Ambler notation.

Table S2.1 MIC of third-generation cephalosporins conferred by BlaC wild-type and mutants

	MIC (μg/mL) for ceftazidime			MIC (μg/mL) for ceftriaxone		
Mutations	23℃	30℃	37℃	23℃	30℃	37℃
WT	<0.5	<0.5	<1	<0.025	<0.025	0.025
F72Y	<0.5	<0.5	0.5	<0.025	<0.025	0.025
S99G	0.5	1.5	0.5	0.025	0.05	0.05
I105F	0.5	1	2	0.025	0.05	0.1
A205T	<0.5	1	1.5	0.025	0.05	0.1
D240G	<0.5	1	1.5	0.05	0.05	0.1
C287Y	0.5	1	1.5	0.05	0.15	0.15
P167S	1.5	2.5	1	0.1	0.2	0.1

Table S2.2. Kinetics fitting parameters for ceftazidime hydrolysis by BlaC P167S.

$C_{substrate}$ (μM)	v_1 (μM/s)	v_s (μM/s)	k (s^{-1})	Relative Burst Amplitude[a]
10	0.0052	0.00032	0.051	0.8
25	0.0071	0.00044	0.049	1.2
50	0.0101	0.00079	0.048	1.8
100	0.0251	0.00075	0.045	5.3
125	0.0530	0.00078	0.039	13.1

[a] The relative burst amplitude is determined by taking the intercept of the 2nd-phase curve and the y-axis (time 0) and dividing it by the enzyme concentration (0.1 μM).

Table S2.3 Chemical shifts of BlaC P167S mutant used in the TALOS+ prediction.

Residues	δ_{HN} (ppm)	δ_N (ppm)	$\delta_{C\alpha}$ (ppm)	$\delta_{C\beta}$ (ppm)	δ_C (ppm)
E165	7.393	112.374	53.836	29.317	174.410
E166	8.207	120.715	58.621	38.607	174.920
S167	8.385	118.198	60.892	63.665	-
E168	8.376	126.713	60.578	29.045	178.434
L169	7.661	116.101	57.568	39.609	-
N170	7.563	119.010	54.700	-	-
R171	7.574	115.809	55.920	31.382	176.277

Table S2.4 Parameters of data collection and refinement for the BlaC P167S crystal structure.

Data collection	8OE5	8OE1
Wavelength (Å)	0.98Å	0.98Å
Resolution (Å)	53.64-1.8 (1.8-1.84)	54.15-1.9 (1.9-1.94)
Space group	P 1	P 1
Unit cell a, b, c (Å)	40.63 53.69 56.27	40.60 54.18 56.04
CC1/2	99.9(86.4)	98.1 (44.6)
Rpim (%)	3.4(68.3)	12.3(71.6)
|I/σI|	14 (2.6)	6.1(1.3)
Completeness (%)	96.0(94.9)	95.4(93.8)
Multiplicity	2.0(2.0)	1.6 (1.6)
Unique reflections	39659	33495
Refinement		
Atoms protein/ligands/water	4038/38/357	3982/40/212
B-factors protein/ligands/water (Å2)	23.4/41.7/31.2	19.3/35.3/27.3
Rwork/R free (%)	16.2/19.3	17.3/20.2
Bond lengths RMSZ/RMSD (Å)	0.44/0.007	0.481/0.007
Bond angles RMSZ/RMSD (°)	0.85/1.49	0.93/1.42
Ramachandran plot preferred/outliers	515/6	514/5
Ramachandran plot Z-score	0.01±0.33	-0.19±0.36
Clash score	4.2	3.4
MolProbity score	1.2	1.2

Table S2.5 Simulated kinetic parameters for ceftazidime hydrolysis in MES buffer by BlaC P167S.

Parameters	
k_1 (μM/s)	0.01
k_2 (s^{-1})	10
k_3 (s^{-1})	1.3
k_4 (s^{-1})	0.0025
k_5 (s^{-1})	5
k_6 (μM/s)	0.01
k_7 (s^{-1})	0.015
k_8 (s^{-1})	0.035
k_9 (μM/s)	0.01
k_{10} (s^{-1})	15
k_{11} (s^{-1})	10
k_{12} (s^{-1})	2
k_{13} (s^{-1})	50
k_{14} (μM/s)	0.1